BIULETYN WAT
ROK XLVI, NR 2, 2000

Growth and characterization of lithium tantalate single crystals doped with Ho, Tm, Nd, Yb, Pr and doped by diffusion with Cr and Cu

SŁAWOMIR MAKSYMILIAN KACZMAREK*
MAREK ŚWIRKOWICZ**
RYSZARD JABŁOŃSKI**, GEORGES BOULON***

*Instytut Optoelektroniki WAT, 00-908 Warszawa, ul. S. Kaliskiego 2 tel. 859037
**Instytut Technologii Materiałów Elektronicznych, 01-919 Warszawa, ul. Wólczyńska 133
***Labortoire de Phys.-Chimie des Materiaux Luminescentes, 69622 Villerbane, Cedex, France

Abstract. Crystal growth conditions for lithium tantalate single crystals doped with rare-earth and conditions of diffusion process for doping with Cr and Cu have been described. Temperature dependencies of conductivity and capacitance were measured and Curie temperature (~610^{o}C) was determined for each crystal. Performed ESR investigations suggest probable localization of impurities incorporated by diffusion at Li^{+} sites, impurities incorporated during growth at Ta^{5+} or interstitial sites and also strong structure deviations in Nd, Yb: $LiTaO_3$ in comparison with to $LiNbO_3$ single crystals. Absorption and additional absorption after γ-irradiation and annealing treatments at room temperature were measured. The γ-irradiation with a dose of 10^5 Gy and subsequent annealing at 800^{o}C in the air for 3 h lead to a valency change of Ho and Pr ions. In the case of γ-irradiation recombination process due to Compton effect seems to be responsible for valency change process in both crystals. Luminescence and radioluminescence measurements in UV+VIS range show a weak excitation energy transfer from $LiTaO_3$ lattice to impurity ions. All studied single crystals reveal good optical quality and higher absorption than in the case of yttrium-aluminate garnets with similar level of rare-earth concentration.

Keywords: crystal growth, absorption, luminescence, additional absorption, electron spin resonance
Symbole UKD:

1. Introduction

Lithium tantalate is one of the promising materials for planar wave-guide lasers for optical telecommunication. Solid state, resistant materials emitting in appropriate wavelength region (1.5 μm) with high efficiency and cheap are needed. Ferroelectric materials are interesting due to a possibility of applying the lasing effect and also non-linear effects in the same specimen. One of the candidates is $LiTaO_3$ with Curie point ca 610^{o}C and trigonal structure used widely as surface acoustic wave substrate, electro-optic modulator and second harmonic generation material [1]. Recently, there have been successful attempts of using Nd: $LiTaO_3$ for a construction of wave-guide laser [2] and also diode-pumped (800 nm) "slab" type laser. For both polarizations, σ and π, output energy was about 10 mW for pump power about 70 mW [3].

The main purpose of this work was to determine the conditions of single crystal growth by the Czochralski method of lithium tantalate doped with rare-earths and measurement of optical properties (absorption, luminescence, additional absorption due to γ-irradiation and thermal annealing) and ESR spectra of obtained crystals. Conditions of thermo-diffusion (temperature and period) for $LiTaO_3$ crystals doped with transition metal ions, Cr and Cu were also found.

2. Experimental procedure

2.1. Charge material

The main problem of $LiTaO_3$ growth is determining the charge composition which leads to axially uniform single crystals. There are many data on compositions melting congruently (from 48.39 mol. % Li_2O: 51.61 mol. % Ta_2O_5 to 48.75 mol. % Li_2O: 51.25 mol. % Ta_2O_5 [4-7]) leading to the most homogeneous single crystals. According to Curie temperature measurement, in this work it has been checked that the best results may be obtained for the following composition:

$$48.75 \text{ mol. \% } Li_2O: 51.25 \text{ mol. \% } Ta_2O_5 \quad (1)$$

All the growth charges were prepared according to this formula starting from Li_2CO_3 of 4N-purity from Institute of Electronic Materials Technology and Ta_2O_5 of 4.5N–purity made in China. Mixed materials were put into Pt container and then heated at 1250^{o}C for 6h. Such solid state reaction gives the only $LiTaO_3$ phase

which was confirmed by X-ray analysis. Dopants (rare-earth oxides) were added to the charge extra.

2.2. Thermal system

For crystal growth iridium crucible 50 mm in diameter and height was used. Two different thermal systems – one with active and other with passive iridium afterheater were prepared and temperature profiles were measured. The systems are presented in Fig. 1.

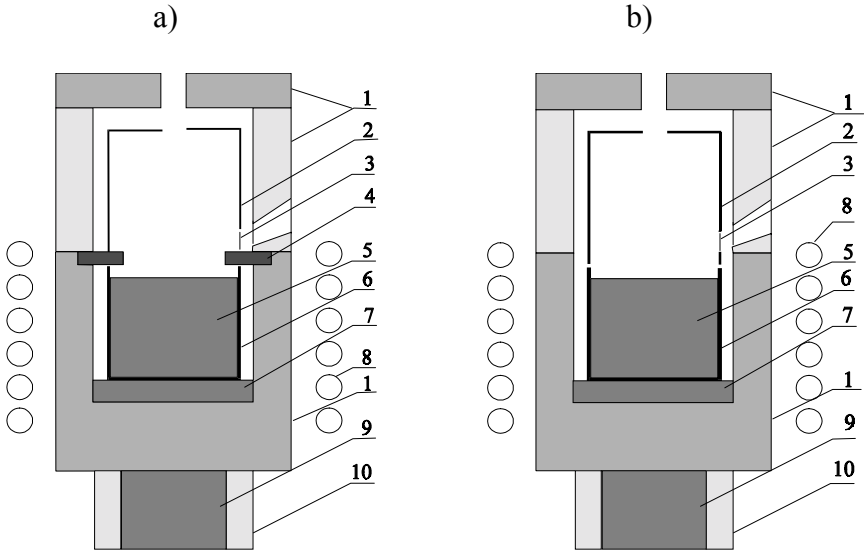

Fig. 1. Thermal system with (a) passive and (b) active iridium afterheater (1 – heat shields of porous aluminum ceramics, 2 – afterheater, 3 – viewing ports, 4 – aluminum ceramics ring, 5 – $LiTaO_3$ melt, 6 – iridium crucible, 7 – zircon grog, 8 – r.f. coil, 9 – ceramic blanket "Kaowool", 10 – aluminum tube)

Axial temperature distributions were measured by Pt6%Rh-Pt30%Rh thermocouple and MTB-2k meter (Thermolab, Poland). In Fig. 2 axial temperature distribution for passive afterheater is depicted. The similar distribution for active afterheater is presented in Fig. 3. Two vertical lines represent crucible edge (0) and the melt surface (-17.5 mm) levels. All measurements were performed in such a way that after melting the temperature of the melt surface was kept close to 1650^{o}C and r.f. power was maintained at corresponding level.

A lowering of temperature near 18 mm for the passive afterheater and at 15 mm for the active afterheater is a result of viewing port in afterheater and heat shields.

According to Figs 2 and 3 it can be estimated that axial temperature gradient near melt surface is equal to 100 K/cm for the passive afterheater but about 50

K/cm for the active one. The two thermal systems give a possibility of adjusting the growth conditions to potential needs.

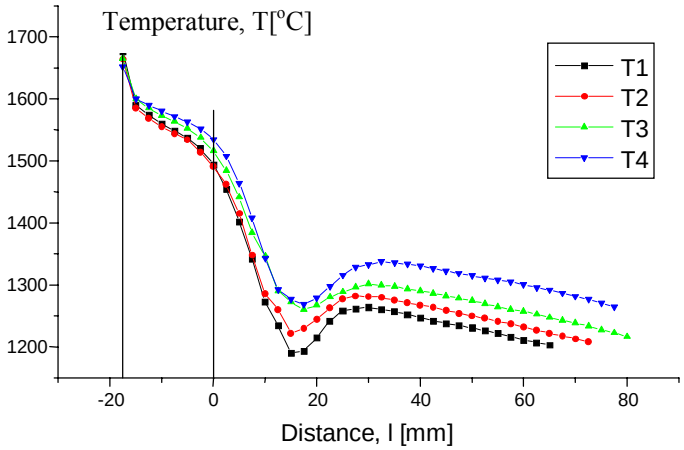

Fig. 2. Temperature distribution for a system with the passive afterheater. T1 – corresponds to crucible edge at the coil top and, by 6 mm shift to T4 which corresponds to crucible edge 18 mm below coil top

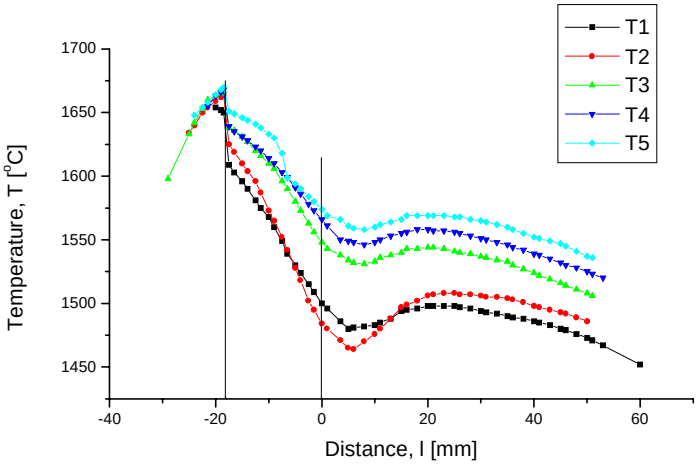

Fig. 3. Temperature distribution for a system with the active afterheater. T1 – corresponds to crucible edge 6 mm above r.f. coil top and consequently by 6mm shift to T5 which corresponds to crucible edge 18 mm below r.f. coil top

2.3 Crystal growth

All melting and crystal growth runs were performed using r.f. heated Czochralski apparatus (MSR-2 made by Metals Research Ltd., England) equipped with computer regulated automatic diameter control unit with Sartorius electronic balance. Single crystals were grown starting from the pre-reacted charge of the formula shown above. Dopants were introduced extra to the charge in the form of oxides of corresponding rare-earth elements. The following elements and concentrations were used: Pr (0.05 at. % and 0.5 at. %), Nd (0.5 at. %), Nd (0.5 at. %) and Yb (0.7 at. %), Tm (0.43 at. % and 0.72 at. %) and Ho (0.3 at. % and 0.5 at. %).

At the beginning undoped single crystals were grown. The conditions were the following: pulling rate – 4 mm/h, rotation rate – 18-20 r.p.m, the active afterheater in T3 position, nitrogen flow 200 ml/min and cooling after growth 24h. Colorless single crystals 18 mm in diameter and 50 mm long were obtained.

Depending on a dopant the pulling rate changed from 0.8 mm/h for thulium to 2 mm/h for praseodymium and rotation rate was in range 10-30 r.p.m. All runs were performed in nitrogen flowing through growth chamber with a rate of 0.2 l/min. After removing crystals from the melt they were cooled down to room temperature for 24h.

In the case of Pr^{3+} doping thermal system with the active afterheater in the position T2 was used. For other dopants the passive afterheater in different positions with respect to r.f. coil turned out to be suitable.

Diffusion of Cr and Cu was performed in Cr_2O_3 and CuO, respectively. The temperature was changed from 750°C to 1100°C. All annealing processes were done in the air.

2.4 Poling of single crystals

After growth all crystals were annealed at 1200°C for 10h in an environment of oxygen flowing with a rate of 1 l/min and then were cooled down to the room temperature for 36h. Poling was performed at temperature T_c+20 °C with current density 0.2-0.3 mA/cm^2. Cooling rate was 30-40 K/h and electric field was switched off at temperature T_c-50 °C. To avoid platinum or silver diffusion into crystals, thin layers of powdered $LiTaO_3$ were used in direct contact with crystal surfaces. There were no observed segregation effects of dopants during poling which was confirmed by Curie temperature measurements of specimens cut off from different parts of crystal before and after poling. Specimens were cut perpendicularly to "c" axis (Z direction) and their surfaces were covered by platinum paste. The Hewlett Packard LCR Meter HP 4263B was used for all Curie temperature measurements.

2.5 Optical measurements

The samples for optical measurements cut out perpendicularly to either Z or Y directions were on both sides polished to the thickness of about 1 mm. The specimens of the following compositions were prepared: $LiTaO_3$ (LT), Pr(0.05 at. %): LT, Pr(0.5 at. %): LT, Nd(0.5 at. %): LT, Nd(0.5 at. %) and Yb(0.7 at. %): LT, Tm(0.43 at. %): LT, Tm (0.72 at. %): LT, Ho(0.3 at. %): LT, Ho(0.5 at. %): LT and Cr: LT and Cu: LT doped by thermo-diffusion (0.6 mm in thick).

The samples were irradiated by gamma photons immediately after the crystal growth process. The ^{60}Co gamma source with a power of 1.5 Gy/sec was used. The gamma doses up to 10^6 Gy were applied.

Optical transmission was measured before and after γ-irradiation and/or annealing treatments using LAMBDA-2 Perkin-Elmer spectrophotometer in UV-VIS range and FTIR-1725 in the IR range. According to measured transmission the absorption was calculated. Additional absorption was calculated according to the formula:

$$\Delta K(\lambda)=(1/d)\ln(T_1/T_2) \tag{2}$$

where K is the absorption, λ is the wavelength, d is the sample thickness and T_1 and T_2 are transmissions of the sample before and after a treatment, respectively.

Fluorescence spectra were obtained in the range of 200-800 nm using Perkin-Elmer spectrofluorimeter LS-5B. Excitation with lasers of wavelength of 355, 442 and 530 nm was also applied.

Radio-luminescence spectra were obtained in the range of 200-850 nm using X-ray excitation (DRON, 35 kV/25 mA) and ARC Spectra Pro-500i spectrograph: ARC Spectra Pro-500i (diffraction grating Hol-UV 1200 gr/mm and diffraction grating brighten up at 500 nm 1200 gr/mm, 0.5 mm slits), PMT: Hamamatsu R928 (1000 V).

2.6 ESR measurements

The dimensions of samples for ESR investigation were following: 3.5x3.5x2 mm. They were investigated by the Bruker ESP300 ESR spectrometer (X-band). The spectrometer was equipped with helium flow cryostat type ESR900, Oxford Instruments. The ESR investigations were performed in the temperature range from 4 to 35 K and microwave power from 0.002 to 200 mW.

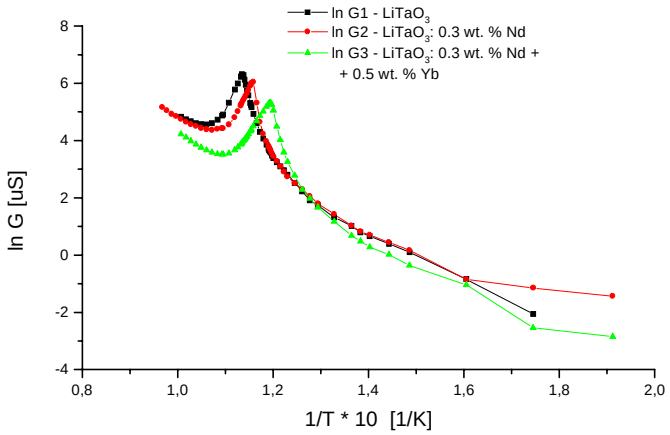

Fig. 4. Temperature dependences of a conductivity for LT, Nd: LT and Nd, Yb: LT single crystals

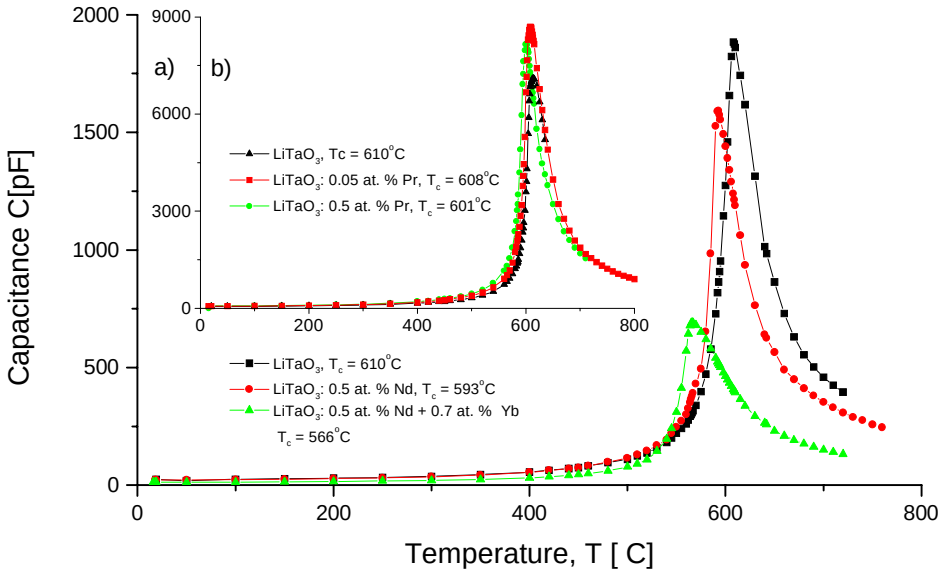

Fig. 5. Temperature dependences of a capacitance for (a) LT, Pr(0.05 at. %): LT, Pr(0.5 at. %): LT and (b) LT, Nd(0.5 at. %): LT and Nd(0.5 at. %) and Yb(0.7 at. %): LT single crystals

3. Temperature dependencies of conductivity and capacitance

In Fig. 4 temperature dependencies of conductivity for LT, Nd: LT and Nd, Yb: LT single crystals are presented. As one can see, Nd, Yb: LT single crystal shows clearly different dependence shows. In Fig. 5 temperature dependencies of capacitance for (a) LT, Nd: LT, Nd, Yb: LT and (b) Pr: LT single crystals are depicted. Nd, Yb: LT single crystal reveals clearly different dependence. Moreover, this crystal shows also different value of measured Curie temperature. For all studied crystals Curie temperature changes within a range of 566-610 ^{o}C and is the lowest for Nd, Yb: LT single crystal. So, Curie temperature measurements are strongly influenced by defects in a crystal.

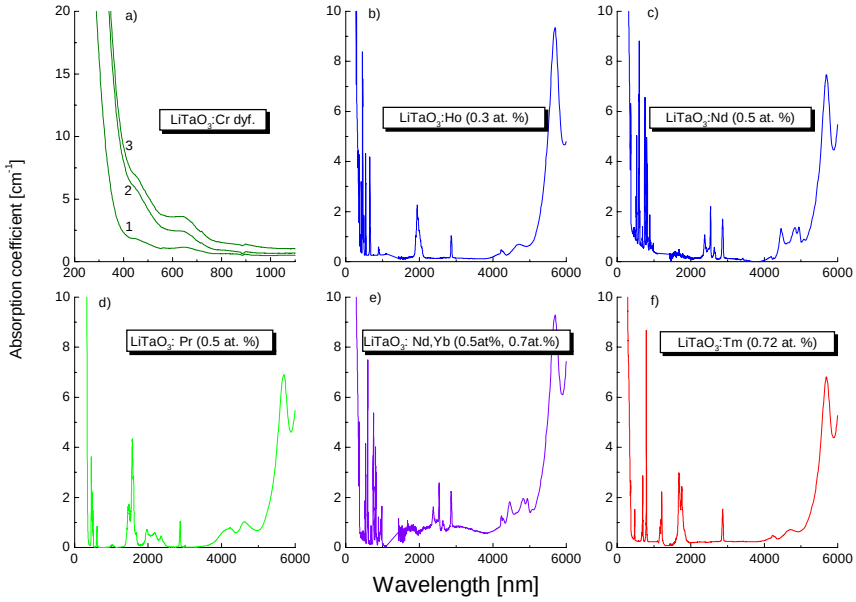

Fig. 6. The absorption of LT crystals: (a) Cr diffusely doped at 900^{o}C for 1 – 5h, 2 – 10h and 3 – 20h, (b) Ho (0.3 at. %), (c) Nd (0.5 at. %), (d) Pr (0.5 at. %), (e) Nd (0.5 at. %) and Yb (0.7 at. %) and, (f) Tm (0.72 at. %)

4. Absorption and additional absorption

The level of defective structure of crystals can be at first approximation estimated by absorption and especially by additional absorption measurements after irradiation with γ-quanta and annealing in an appropriate atmosphere. It is involved in absorption value (optical density of a crystal) and additional absorption bands (their shape and position which suggest color centers appearing due to particular treatment).

The optical absorption of LT crystals doped with Cr, Ho, Nd, Pr, Nd and Yb and Tm is presented in Fig. 6. Chromium was introduced into single crystalline plate by thermo-diffusion at 900^{o}C with annealing periods 5, 10 and 20 h (Fig. 6a)

It can be seen that single crystals doped with Nd and Yb (Fig. 3 e) are characterized by the highest optical density. The fundamental absorption edge in the case of Cr diffusive doping is equal to 267 nm, so it is the same as for undoped material and independent on dopant concentration. In the case of crystals doped during growth the absorption edge shifts to about 275 nm except Pr (0.5 at. %): LT crystal when it is equal to 320 nm.

It should be emphasized that absorption caused by rare-earth ions is higher for LT single crystals than for yttrium-aluminum garnet (YAG) with the same doping level.

In the absorption spectrum of LT single crystals doped during growth there arise very clear band due to an existence of OH^- ions in the lattice (Fig. 6b-f, 2871 nm band). It suggests that rare-earth ions are located in LT lattice in another positions than Li^+ sites. In the case of doping by diffusion with Cr or Cu only weak absorption is observed near wavelength corresponding to OH^- line. The mentioned observations suggest that location of active ions depends on the method of doping. In the case of doping by thermo-diffusion a decrease of intensity of OH^- absorption bands leads to conclusion that ion dopants are introduced into Li^+ sites in LT lattice. On the other hand, doping during growth probably leads to an incorporation of active ions into Ta^{5+} sites or interstitial positions with octahedral symmetry. Incorporation of dopants into Li^+ sites during thermo-diffusion can be explained in the following way. It is evident that in LT single crystals obtained from the congruently melting composition the principal defects are lithium vacancies. During diffusion process at elevated temperatures dopant ions occupy these vacancies. For crystals doped during growth other positions in LT lattice (e.g. Ta^{5+}) are energetically more favorable.

The OH^- absorption band in diffusely doped LT single crystals is broader than in crystals doping during growth which suggests that they are more defected.

In Fig. 7 an additional absorption of LT single crystals (a) diffusely doped with Cr (curves 1 and 2) and Cu (curve 3), (b) undoped (curve 4) and doped during growth (curve 5) is presented. As one can see, after γ-irradiation in lithium tantalate single crystals, independently on dopant, additional absorption bands appear with maxima at wavelengths: 311, 394 , 2871 and 4200 nm. In the first band region crystal is brighten up, the second is connected with color center, the third is due to a change in OH^- concentration and the fourth could be connected with f-f transitions. Observations of changes in absorption of diffusely doped crystals suggest that an intensity of the first band is in the same way related to defective level connected with doping process. Moreover, in undoped LT and Nd: LT single crystals there arises also broad band in the range 500-900 nm.

The factors limiting diffusion process for LT crystals doped by diffusion are temperature and period. In temperatures lower then 900°C diffusion process is slower, moreover in shorter period the amount of impurity entering the crystal is lower and crystal shows a higher defective level. Comparison of 1, 2 and 3 curves shows that diffusion is more effective for Cr than for Cu ions.

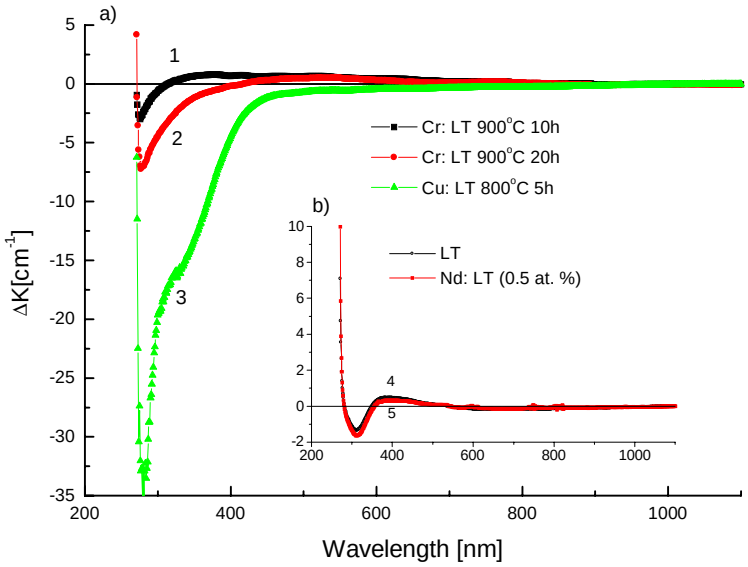

Fig. 7. The additional absorption of LT single crystals after γ-irradiation: (a) diffusely doped with Cr (curves 1 and 2) and with Cu (curve 3) – doses 10^5 Gy and, (b) undoped (curve 4) and doped during growth with Nd (curve 5) – doses 10^6 Gy

In the case of LT crystals doped during growth with Nd the level of defective structure is lower than for diffusive doping and also lower than for undoped LT single crystals.

Fig. 8 presents the additional absorption after γ-irradiation with a dose of 10^5 Gy in other specimens of LT crystals doped during growth (curves 1-5 for Nd and Yb, Pr, Pr, Ho, Ho, respectively and Tm (curve 8) in comparison with undoped (curve 6) and Nd: LT specimens (curve 7) irradiated with a dose of 10^6 Gy.

It can be observed that single crystal Pr(0.05 at. %): LT is characterized by the highest additional absorption in the band 394 nm (curve 2). The material, due to shallow minimum at 311 nm, is probably also characterized by the lowest level of defective structure connected with doping. An increase of praseodymium content leads to an improvement of LT lattice structure and additional absorption decreases (curve 3).

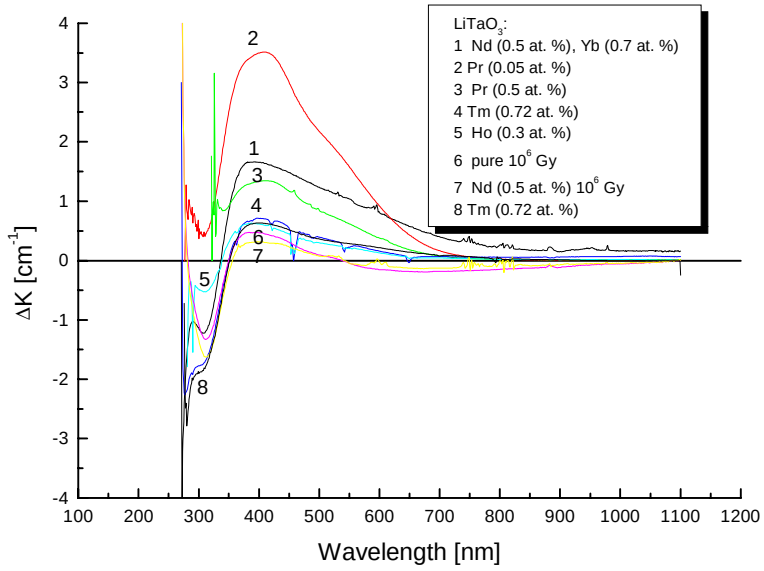

Fig. 8. An additional absorption after γ-irradiation in LT single crystals doped with (1) Nd and Yb, (2 and 3) Pr, (4 and 5) Ho, (7) Nd, (8) Tm and, in (6) pure one. The last two crystals were irradiated with a dose of 10^6 Gy, while others with 10^5 Gy.

The similar effect has been observed for yttrium aluminum perovskite (YAP) single crystals doped with praseodymium [8]. As it was confirmed by Curie temperature measurements for samples cut from the origin and the end of the crystal (changes about ±2 K in Curie temperature at the accuracy of ±1 K), the crystals showed uniform longitudinal impurity distribution. Also X-ray probe measurements stated uniform praseodymium distribution. On the base of these measurements one can say that Pr segregation coefficient in LT crystal is nearly equal to 1.

The highest amount of point defects exists in Nd, Yb: LT crystals (curve 1); there is a deep minimum at 311 nm and large value of additional absorption at 394 nm. Doping with Tm (curve 8) and Ho (curves 4 and 5) leads to similar results in additional absorption, with exception of characteristic bands for Ho: LT crystals caused by transitions in Ho^{3+}. Perhaps it is a result of valency change of Ho ions due to γ-quanta irradiation; probably Ho^{3+} ions capture Compton electrons and become divalent.

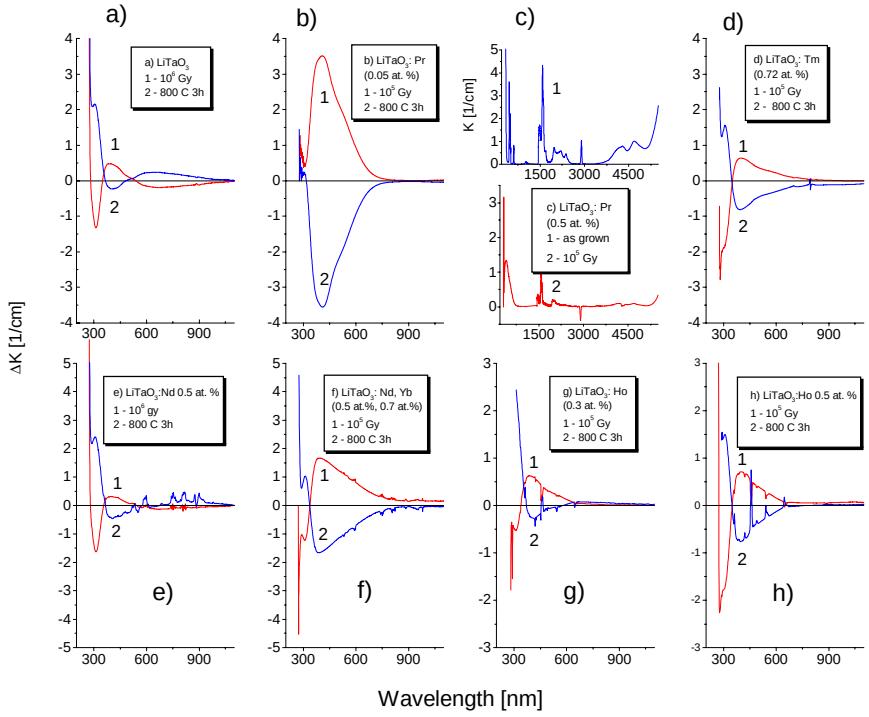

Fig. 9. An additional absorption of lithium tantalate single crystals after successive irradiation and annealing at 800°C in air for 3h

The change in valency of Ho ions is clearly seen in Fig. 9g and h where an additional absorption after γ-irradiation is depicted with an additional absorption after annealing the irradiated crystals at 800°C in air for 3h. The annealing leads to a valency change of Ho ions in the opposite direction ($Ho^{2+} \rightarrow Ho^{3+}$).

Similarly as for Ho: LT, Pr: LT single crystals show also valency changes of Pr ions after γ-irradiation. In this case in IR range of absorption spectrum an

additional absorption characteristic for intra-atomic transitions in Pr is observed (Fig. 9c). It can be an effect of a capture of Compton electron by Pr^{4+} ions existing in the crystal which become trivalent. According to Fig. 9c, valency change of Pr ions is accompanied by a decrease in OH^- concentration (2871 nm band) and depends on Pr starting concentration. Moreover, valency changes of Ho and Pr ions are accompanied by changes in value of the absorption after γ-irradiation which are observed in the far infrared (a band close to 4200 nm).

According to Fig. 9 an annealing at 800°C for 3h in the air almost completely removes an additional absorption caused by γ-irradiation in LT single crystals doped during growth.

In Fig. 10a changes in absorption of Ho(0.5 at. %): LT single crystals after defined treatments are presented. According to the results, the irradiation with γ-quanta (curve 2) decreases Ho^{3+} ion concentration (negative value of additional absorption), in turn, an annealing of irradiated specimen at 800°C in the air leads to an increase of this concentration (curve 3). It suggests that γ-irradiation is responsible for valency change $Ho^{3+} \rightarrow Ho^{2+}$ as a result of Compton electron capture. The curve 4 represents an absorption change of the specimen after annealing at 1300°C for 1h in hydrogen (in Fig 10b it is depicted for broad wavelength range). In this case valency changes are not evident, probably the annealing temperature has been very high and there were changes in two opposite directions (an increase and a decrease in valency).

Fig. 10. (a) The absorption (curve 1) and additional absorption (curves 2-4) in Ho doped LT single crystals after successively: γ-irradiation with a dose of 10^5 Gy (curve 2), an annealing at 800°C for 3h in air (curve 3), an annealing at 1300°C for 1h in hydrogen (curve 4) in the wavelength range 400-500 nm and (b) the additional absorption in Ho: LT single crystals after annealing at 1300°C for 1h [illegible] length range 200-500

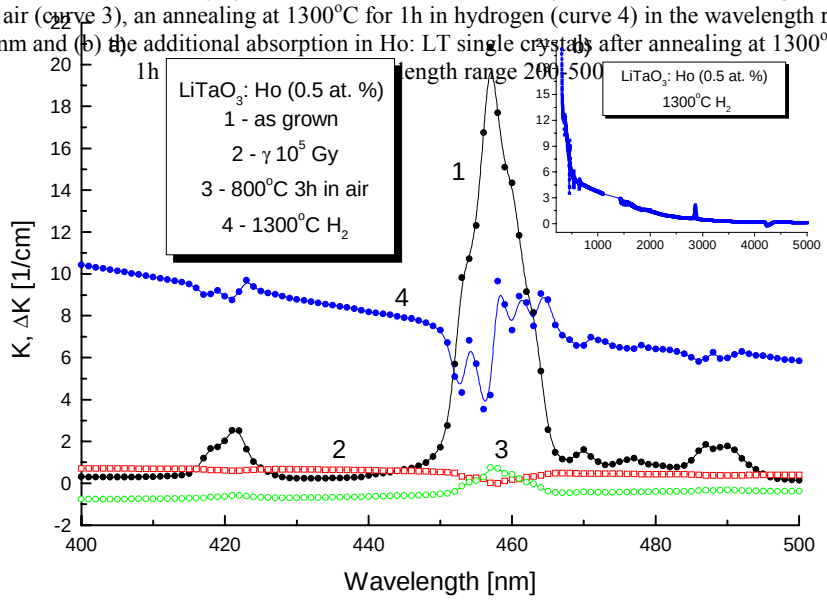

In Fig. 10b an increase in absorption close to 2871 nm band and a decrease near 4200 nm are clearly seen.

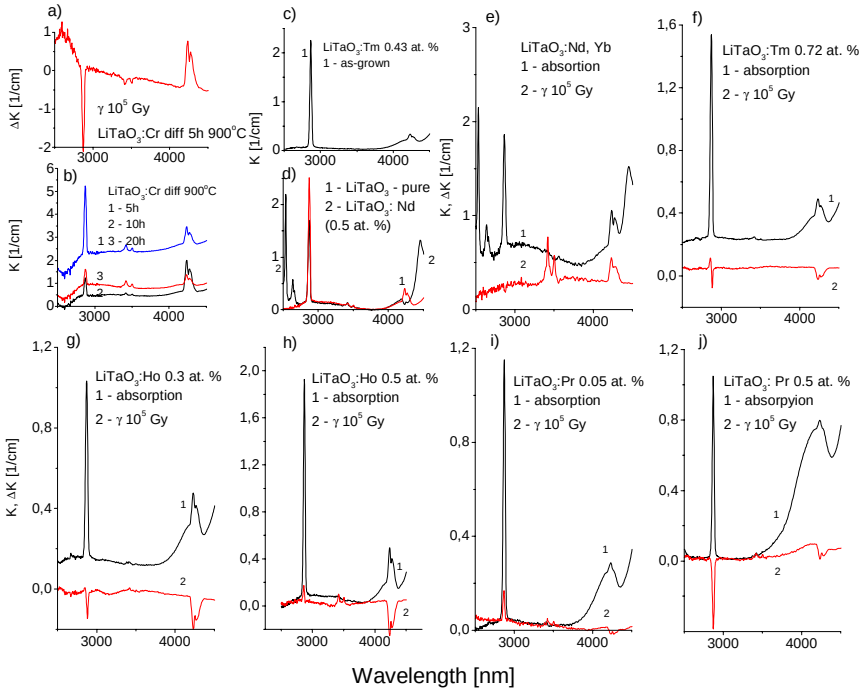

Fig. 11. The absorption and additional absorption of LT single crystals in near infrared region: (a and b) – crystals diffusely doped with Cr, (c) - Tm (0.43 at. %): LT, (d) – undoped (curve 1), Nd(0.5 at. %): LT (curve 2), (e) – Nd and Yb: LT, (f) – Tm (0.72 at. %): LT, (g) – Ho(0.3 at. %): LT, (h) – Ho(0.5 at. %): LT, (i) – Pr(0.05 at. %): LT and (j) – Pr(0.5 at. %): LT

In Fig. 11 the absorption and additional absorption after γ-irradiation with a dose of 10^5 Gy for undoped and Cr, Tm, Nd, Nd + Yb, Ho and Pr doped LT single crystals in the wavelength range of 2500-4500 nm are presented. Very high absorption peaks (in comparison with LN single crystals) are observed at 2871 nm which indicates an existence of OH^- group. The absorption changes in diffusely doped crystals suggest that dopant ions are incorporated into Li^+ sites in the LT lattice. The conclusion is confirmed by Fig. 11a, where a decrease in absorption with the wavelength is observed after γ-irradiation for crystals diffusely doped with Cr. According to Figs 11 c, f and h, Tm and Ho ions are located in lattice sites different than Li^+ sites. The other dopants enter into Li^+, Ta^{5+} sites and also into

interstitial positions. It depends on dopant concentration too (see Fig. 11 g, h for Ho and Fig. 11 i, j for Pr).

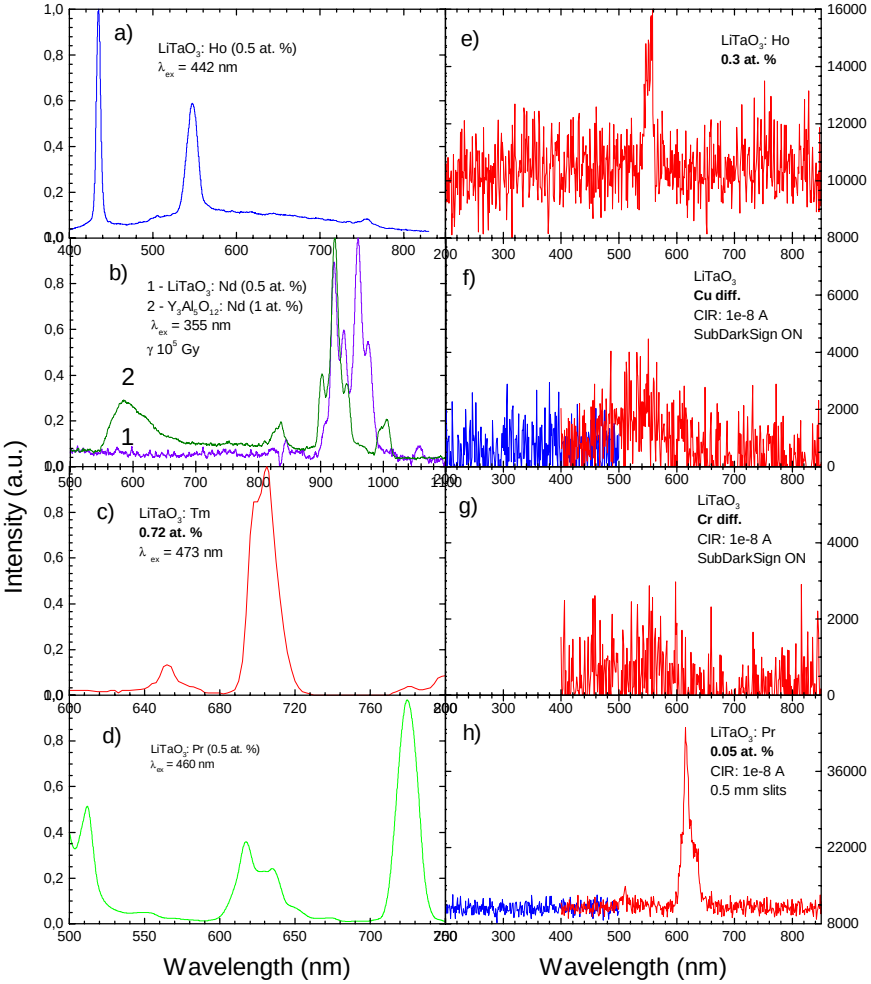

Fig. 12. (a-d) Uncorrected luminescence spectra of Ho(0.5 at. %): LT, Nd(0.5 at. %): LT, Tm(0.72 at. %): LT and Pr(0.5 at. %): LT, respectively and (e-h) radioluminescence spectra of Ho(0.3 at. %): LT, Cu(dif.): LT, Cr(dif.): LT and Pr(0.05 at. %), respectively

In comparison with lithium niobate, an additional absorption for LT single crystals (0.45 cm^{-1} for 394 nm band) is similar in value and a shape and its lower value for doping by diffusion Cr crystals suggests that chromium can be introduced into lithium tantalate easier than to lithium niobate. Probably 394 nm band corresponds to 385 nm band for lithium niobate, which is caused by F centers [9].

The 311 nm band has no equivalent band in LN spectrum but similar kind of brightening is observed for LN crystals near 350 nm [10].

Negative change of 2871 nm band after γ-irradiation indicates that there takes place a change in defective structure of LT crystal, which may be an increase in dopant ions concentration in Li^+ sites. Positive change of 2871 nm band after γ-irradiation may indicate a decrease in dopant concentration in Li^+ sites. So γ-irradiation significantly changes defective structure of LT single crystal.

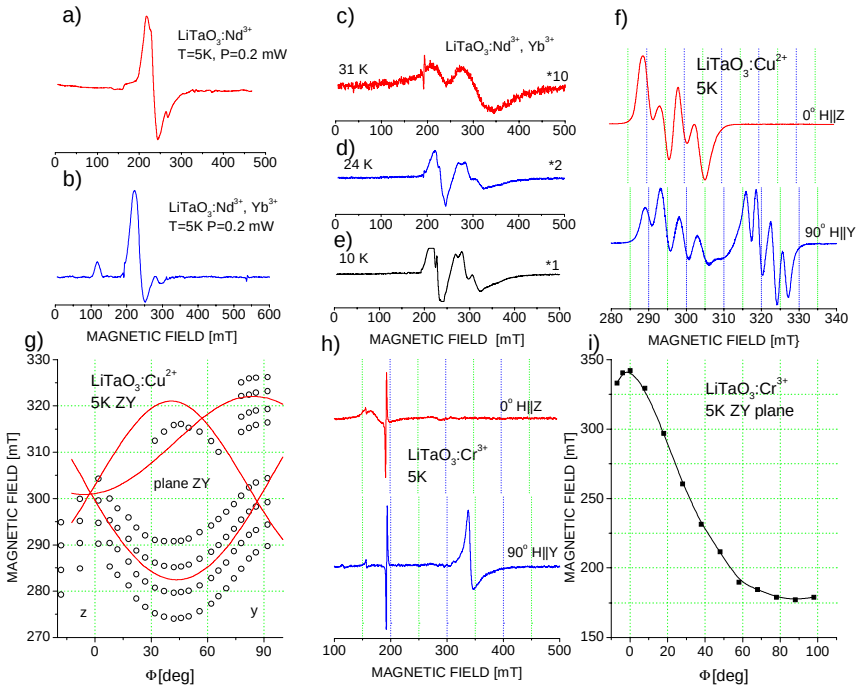

Fig. 13. Derivative ESR spectrum of polycrystalline (a) Nd: LT and (b) Nd, Yb: LT, ESR spectrum of single crystal Nd, Yb: LT for (c) 31K, (d) 24 K and (e) 10K, (f-i) ESR spectra of crystals doped by diffusion: (f) Cu: LT for H||Z and H||Y, (g) angular dependence for Cu: LT – circles–experiment and solid lines-calculated values for the centers of hyperfine lines, (h) Cr: LT for H||Z and H||Y and (i) angular dependence for Cr: LT in ZY plane

5. Luminescence and radioluminescence measurements

In Fig. 12 luminescence (a-d) of LT single crystals doped with: (a) Ho(0.5 at. %), (b) Nd(0.5 at. %), (c) Tm (0.72 at. %) and (d) Pr (0.5 at. %) and radioluminescence (e-h) of diffusely doped LT crystals with (f) Cu and (g) Cr and doped during growth (e) Ho (0.3 at. %) and (h) Pr (0.05 at. %) measurements are

presented. The crystals doped diffusely show a weak luminescence and do not show any radioluminescence bands. Among all studied crystals only Ho: LT (550 nm band) and Pr: LT (620 nm band) reveal clear radioluminescence spectrum. It may indicate that in LT single crystals excitation energy transfer from lattice to impurity ions is rather weak.

Among crystals doped during growth clear luminescence bands show: in VIS range - Ho: LT (550 and 760 nm bands), Tm: LT (652 and 705 nm bands), Pr: LT (515, 620 and 720 nm bands) and Nd (1 μm) in IR range.

6. Electron spin resonance

ESR spectra were measured for all crystals under test. Moreover ESR spectra for powdered Nd: LT and Nd, Yb: LT single crystals were done.

In Fig 13 a and b polycrystalline spectra of Nd: LT and Nd, Yb: LT crystals are depicted. They are presented due to a problem of separating Nd and Yb lines in Nd, Yb: LT single crystals. As one can see from Fig. 13c, d and e ESR spectrum of Nd, Yb: LT single crystal is, unfortunately, isotropic. It may indicate that Nd, Yb: LT single crystal is strongly defected due to e.g. competition of Nd and Yb ions in substituting of lattice sites. Such conclusion is confirmed by absorption spectra measurements of Nd and Yb doped LN and LT single crystals. In the first case strong absorption of Yb ions is observed in the absorption spectrum, while in the second case this absorption is weak.

Figs 13 f -i show ESR spectra for diffusely doped (f and g) Cu: LT and (h and i) Cr: LT crystals. The lines presented in these Figs are anisotropy and measured for the following angles: 0^o (H||Z) and 90^o (H||Y). Their angle dependencies are depicted in Figs g and i for Cu: LT and Cr: LT, respectively. For Cu: LT crystals, we have four characteristic for Cu^{2+} ion lines of hyperfine structure (I=3/2). Effective electron spin Hamiltonian one can write as:

$$H = \beta \cdot \mathbf{g} \cdot \mathbf{H} \cdot \mathbf{S} + A \cdot \mathbf{I} \cdot \mathbf{S} \tag{3}$$

where: S=1/2, $H_{res}=\nu/(g\beta/h)$, β is the Bohr magneton, θ is the angle between magnetic field and z-axis, h is the Planck constant, g is the Lange factor, ν is the microwave frequency, H_{res} is the resonance magnetic field and:

$$g^2 = g_x^2 l^2 + g_y^2 m^2 + g_z^2 n^2$$

l, m., n direction cosines, I – nucleus spin, A – hyperfine structure constant.

The values of hyperfine A constant ($A \cdot 10^{-4}$ cm^{-1}) and g_x, g_y and g_z calculated in that paper were compared with literature data on $LiNbO_3$: Cu^{2+} in Table 1.

Table 1

Hyperfine A constants ($*10^{-4}$ cm^{-1}) and Lande factor values for Cu^{2+}: LT as compare to Cu^{2+}: LN crystal [11]

$LiNbO_3$: Cu^{2+} [11]		$LiTaO_3$: Cu^{2+}	
g_x=2.076(5)	A_x=50.5(1)	g_x=2.08(2)	A_x=32.15(5)
g_y=2.106(5)	A_y=30.2(1)	g_y=2.10(2)	A_y=65.5(2)
g_z=2.381(5)	A_z=78.0(1)	g_z=2.43(5)	-

Angle dependencies for lithium tantalate crystal diffusely doped with Cr (Fig. 13 i) show single line, which can be described using the following electron spin Hamiltonian:

$$H=g\cdot\beta\cdot\mathbf{H}\cdot\mathbf{S} \qquad (4)$$

where S=1/2. Calculated values of the Lande factor are as follows: $g_{\|}$=1.9660 and $g_{\perp}$=3.7595.

From the above angle dependencies do not result that Cu^{2+} or Cr^{3+} ions substitute Li^{+} sites only. Kobayashi et al. [11] suggest that they substitute simultaneously Li^{+}, Ta^{5+} and interstitial sites.

7. Conclusions

Temperature distributions and gradients of a temperature were determined for thermal systems with active and passive iridium afterheaters. In order to obtain the high quality crystals thermal system should be adequately chosen. In all crystal growth runs both types of thermal systems were successively applied.

From temperature dependencies of conductivity and capacitance of rare-earth doped LT single crystals it results that Curie temperature clearly depends on the kind of a dopant and also on the level of crystal defecting. Among all crystals under test Nd and Yb doped LT crystals show clearly different temperature dependence for both conductivity and capacitance than others. Absorption measurements confirmed this observation. Nd, Yb: LT single crystal reveals higher optical density. It may be due to a competition between Nd and Yb in substituting LT lattice sites. Such competition is not observed for Nd, Yb: LN single crystals.

In the case of crystals doped during growth the fundamental absorption edge (FAE) is equal to about 275 nm except Pr (0.5 at. %): LT crystal, where it is as high as 320 nm. The FAE in the case of Cr: LT crystal doped by diffusion is equal to 267 nm, so it is the same as for undoped material and is independent on dopant

concentration. Cu doped crystals show some dependence of the FAE on dopant concentration.

In the absorption spectrum of LT single crystals doped during growth there arises a very clear 2871 nm band due to an existence of OH^- ions in the lattice. It suggests that rare-earth ions are located in LT lattice in other positions than Li^+ sites. In the case of doping by diffusion with Cr or Cu only weak absorption is observed near wavelength corresponding to OH^- line. The mentioned observations suggest that location of active ions depends on the method of doping. In the case of doping by thermo-diffusion a decrease of intensity of OH^- absorption bands leads to the conclusion that ion dopants are introduced into Li^+ sites in LT lattice. On the other hand, doping during growth probably leads to an incorporation of active ions into Ta^{5+} sites or interstitial positions.

In the case of Pr doped LT single crystals it seems that for low concentrations of Pr, Pr ions substitute Ta^{5+} or interstitial sites (it is confirmed by high additional absorption after γ-irradiation), while for high concentrations they locate mainly at Li^+ positions.

For crystal doped diffusely with Cu and Cr transition metal ions the main factors determining thermo-diffusion process are temperature and period. The optimum conditions for obtaining good LT crystals doped by diffusion was temperature equal to about 900^{o}C and period about 20 hours.

Additional absorption of LT single crystals after γ-irradiation reveals four bands with maxims at 311, 394, 2871 and 4200nm. Intensity of the first band is in same way related to defective level connected with doping process, the second is connected with color F-type center, the third is due to a change in OH^- ions concentration and the fourth could be connected with f-f transitions. The shallower is the first band the better is impurity incorporation into a crystal. Negative change of 2871 nm band after γ-irradiation may indicate that a change in defective structure of LT crystal takes place, namely an increase of dopant ions concentration in Li^+ sites (e.g. high doped Pr: LT crystal). Positive change of this band may indicate an increase of dopant ions concentration in Ta^{5+} or interstitial sites (e.g. low doped Pr: LT crystal).

Valency change of Ho and Pr ions after γ-irradiation was stated for Ho: LT and Pr: LT single crystals. It was confirmed by changes in absorption observed after annealing of the crystals in air. Probably the following recombination reactions due to Compton electrons take place: $Ho^{3+} \rightarrow Ho^{2+}$ and $Pr^{4+} \rightarrow Pr^{3+}$.

References

1 – E.J. Lim, M.M. Fejer, and R.L. Byer, *Electron. Lett*. 25, 174 (1989)

2 – A. Cardova-Plaza, M.J.F. Digonnet, R.L. Bayer, and H.J. Shaw, *IEEE J. Quantum Electron*. QE-23, 262 (1987)

3 – K.S. Abedin, M. Sato, H. Ito, T. Maeda, K. Shimamura and T. Fukuda, „Ordinary and extraordinary continuous wave lasing at 1.092 and 1.082 μm in bulk Nd: $LiTaO_3$ crystal", *J. Appl. Phys*., 78 (2) (1995) 691

4 – R.I. Barns, J. R. Carruthers, "Lithium tantalate single crystals stoichiometry", *J. Appl. Crystallography*, 3 (1970) 395

5 – H. Iwasaki, S. Miyazawa, T. Yamada, N. Uchida, N. Niizeki, "Single crystal growth and physical properties of $LiTaO_3$", *Rev. Elec. Lab*. 20 (1972) 129

6 – C.D. Bandle, D.C. Miller, "Czochralski growth of large diameter $LiTaO_3$", *J. Cryst. Growth*, 24/25 (1974) 432

7 – P.F. Bordui, R.G. Norwaad, C.D. Bird, and J.T. Carella, "Stoichiometry issues in single crystal lithium tantalate", *J. Appl. Phys*. 78 (1995) 4647

8 – S.M. Kaczmarek, „Role of the type of impurity in radiation susceptibility of oxide compounds", Crystal Research and Technology, 34 (1999) 737-743

9 – S.M. Kaczmarek, R. Jabłoński, I. Pracka, M. Świrkowicz, S. Warchoł, "Radiation defects in $LiNbO_3$ single crystals doped with Cr^{3+} ions", *Crystal Research and Technology*, vol. 34 (1999) 729-735

10 - I. Pracka, A. Bajor, S.M. Kaczmarek, M. Świrkowicz, B. Kaczmarek, J. Kisielewski, T. Łukasiewicz, „Growth and characterization of $LiNbO_3$ single crystals doped with Cu and Fe ions", *Crystal Research and Technology*, vol. 34 (5-6) (1999) 627-634

11 – T. Kobayashi, K. Mutto, J. Kai and A. Kawamori, "ESR and optical studies of $LiNbO_3$ doped with Cu^{2+} ions", *J. Mag. Res*. 34 (1970) 459-468

Wzrost i charakteryzacja monokryształów $LiTaO_3$ domieszkowanych objętościowo Ho, Tm, Pr, Nd, Yb oraz dyfuzyjnie Cr i Cu

Streszczenie. Opracowano warunki krystalizacji tantalanu litu domieszkowanego objętościowo jonami z grupy ziem rzadkich oraz warunki procesu dyfuzji w przypadku domieszkowania jonami z grupy metali przejściowych. Wyznaczono temperaturowe zależności przewodności i pojemności, określając dla każdego kryształu temperaturę Curie. Przeprowadzono badania EPR, z których wynika lokalizacja domieszek wprowadzanych dyfuzyjnie w położeniach głównie Li^+. Wyznaczono absorpcję tych kryształów w temperaturze pokojowej oraz zmierzono dodatkową absorpcję po ich naświetleniu kwantami gamma, a także ich luminescencję i radioluminescencję. Naświetlanie kwantami gamma oraz kolejno wygrzewanie w temperaturze 800^{o}C wykazały zmianę walencyjności jonów Ho oraz Pr. Badane kryształy wykazywały wysoką jakość optyczną. Absorpcja tych kryształów była wyższa aniżeli kryształów YAG z porównywalną koncentracją domieszki.